Computer Simulations of Radiation Shielding Materials for Use in the Space Radiation Environment

A thesis submitted in partial fulfillment of the requirement
for the degree of Bachelor of Science in Physics
from the College of William and Mary in Virginia,

by

Christopher A. O'Neill

Accepted for _____

_____
Advisor: Dr. W. J. Kossler

_____
Dr. John Delos

Williamsburg, Virginia
May 2006

Abstract

This research has involved computer modeling of radiation shielding materials in the space radiation environment. Work has included modeling materials with transport codes developed by NASA-Langley for evaluating their radiation shielding effectiveness. Furthermore, this research has involved starting to make our own transport code based on GEANT4, which will hopefully duplicate the results found using the NASA codes. There have been some promising results found so far, where the results are shown to have good agreement in certain conditions. Hopefully, future work will be able to provide even more agreement between the two models.

Acknowledgements

I would first like to thank Dr. Kossler for his invaluable help with this research by serving as my advisor and his constant willingness to meet with me and explain concepts. I would also like to thank Dr. Steve Blattnig and Dr. Steve Walker, both of whom are at NASA-Langley, for their help with the NASA codes, without which this project would not have been completed. I would also particularly like to Dr. Klaus Grimm for his willingness to explain GEANT4 to me and for donating a code, which is used for recording data. Lastly, I would like to thank the examining committee for their time spent in reading about this research and attending the defense.

Table of Contents

Introduction

NASA has always had a major emphasis on developing technologies that can be used for manned space flight. This has been evidenced by the massive attention that was given to the first manned lunar landing in 1969. This interest in space exploration by the general population has continued to fuel the design of other manned projects such as the Space Shuttle and the future Crew Exploration Vehicle (CEV). Clearly, any sort of manned space flight requires extraordinary design considerations and extremely effective technology, because there are innumerable hazards associated with manned space flight. Among these, radiation damage is a very major concern (1).

The space radiation environment is potentially extremely hazardous. Particulate radiation in space can consist of every known particle including all energetic ions (2). This radiation can be grouped into three major categories. First, there is radiation of galactic origin referred to as Galactic Cosmic Rays or GCR. GCR is a relatively constant background level of radiation throughout the solar system. The GCR spectrum consists of a relatively large number of heavy ions, which is important for estimating radiation damage in biological systems, since these heavy particles cause more damage than a proton of comparable energy. Next, radiation that originates from the acceleration of the solar plasma is referred to as Solar Energetic Particles, SEPs, or Solar Particle Events, SPEs. These SPEs consist almost entirely of protons with a very small number of helium nuclei mixed in. SPEs generally have particles of lower energy than GCR, but they can be extremely dangerous due to the shear number of particles associated with a typical SPE. SPEs can deliver lethal doses of radiation in an extremely short period of time, such as a few days (2). Lastly, radiation particles can be trapped inside the confines of a

geomagnetic field. Around Earth, the bands of trapped particles are referred to as the Van Allen Belts. The Van Allen Belts are a torus of trapped radiation, consisting mostly of protons and electrons centered on the earth's geomagnetic equator. There are two major belts in the Van Allen Belts. The inner belt reaches a maximum at approximately 3,600 km, while the outer belt reaches a very broad maximum at approximately 10,000 km. There is a minimum at around 7,000 km. The inner and outer belts can be potentially harmful to spacecraft leaving Low Earth Orbit (LEO) for interplanetary space. However, usually the passage time is relatively short and so the probability for radiation damage is significantly reduced (2).

Previously, NASA was not too concerned about GCR, since manned missions beyond the van Allen belts were short. NASA was far more worried by SPEs, since they could be lethal in a short period of time and also because SPEs are far more erratic than the GCR spectrum, which only slowly changes (2).

However, with the possibility of long-term deep space missions at hand, NASA must conquer the new challenge of protecting astronauts from the risks of GCR damage. GCR ions significantly increase the risk of cancer and NASA will not accept higher than a 3% risk of a fatal cancer over the lifetime of the astronaut (1). Furthermore, NASA must prevent radiation sickness, which can have effects that compromise mission safety (1). Also, adequate protection from GCR for a prolonged manned mission will most likely provide sufficient protection from a SPE unless the astronaut is engaging in Extravehicular Activity (EVA) (2).

In the GCR spectrum, a large component of the damage is from ions of high charge and energy (HZE), for which unfortunately significant data are lacking on

biological damage. Furthermore, there is not very high accuracy in the cross sections databases for HZE. All of the calculations performed by NASA use nuclear models of the cross section that are checked by comparison with experiment. However, there are large systematic errors in the experiments, which limit the level of confidence in the models (2).

HZE ions passing through materials cause much more damage as they create a larger swath of damaged area, since the energy deposited by charged radiation goes as the square of charge. This can be seen in figure 1(2).

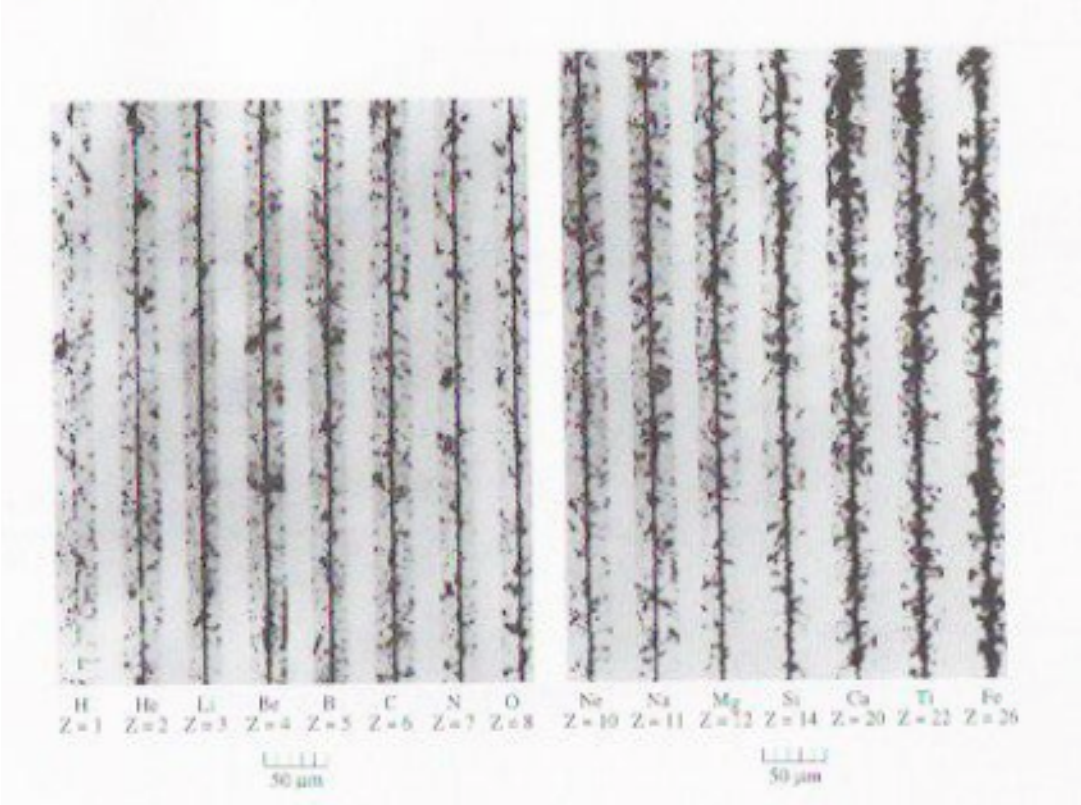

Figure 1. Different Ions of Equal Energy Passing through Material

Figure 1 shows a path of equal energy ions with hydrogen on the far left and iron on the far right. The black represents areas that have been significantly affected or damaged by the ion passing through. As you can see, the cross sectional area of the damage increases

with increasing atomic charge. This shows that ions of equal energy do not necessarily impart the same amount of damage to a system, since it is heavily dependent on the atomic charge. It would take several hundred protons to equal the damage from one iron ion of the same energy. Furthermore, the thickness of the damaged area from an iron ion is sufficiently large that it could destroy the nucleus of a cell, which would constitute a lethal event for that cell. This exemplifies the difficulty in predicting biological damage, since one must be able to predict statistically where in the cell the damage is done. Destruction of the nucleus is fatal for the cell, but destruction of more peripheral components may not be so devastating. Due to this difficulty in modeling an exact biological system, NASA is most interested in limiting the exposure to radiation damage in tissue, which is often approximated as water. Water is used, since a typical cell is between 60% and 90% water by weight. Therefore, water can be considered a very crude biological approximation for radiation damage. To measure this biological damage, dose equivalent is used as a measure of the biological damage from a dose of a certain type of radiation. Dose equivalent is obtained by multiplying the dose by a quality factor, which reflects the expected level of biological damage. Therefore, an iron HZE ion would have a much higher quality factor than a proton, which would show that the iron ion does far more biological damage (2).

It is also important to gain some understanding of what types of materials form effective shields against space radiation. The effectiveness of the radiation shielding material depends on the basic atomic and/or molecular cross sections and also the nuclear cross sections. The atomic and molecular cross sections depend on the density of electrons per unit volume, the electronic excitation energy, and also the tight binding

corrections of the inner shell electrons (3). The best absorbing materials, which make the most effective radiation shielding materials, have the highest electron density, the least electronic excitation energy, and the smallest tight binding corrections (3). Therefore, liquid hydrogen is the best space radiation shielding material (3). Of the three major factors, the single most important feature is the electron density. Therefore, hydrogen will always have the best shielding characteristics of any atom, since it has the highest electron density of any atom. This shows the importance of designing materials that have high hydrogen content. Also, one wishes to have some level of fragmentation of the HZE ions into smaller ions, which are easier to shield against and reduce the quality factor for that type of radiation. Therefore, it is advantageous to have a shielding material that causes some level of fragmentation of HZE ions to make them easier to handle without causing additional secondary particles through fragmentation of the shielding material nuclei (4). Hydrogen again serves this purpose very well, since it cannot fragment into another nucleus. However, if one causes too much fragmentation, then it can be problematic, since there are vastly more particles that must be dealt with. In addition, due to the expense and difficulty in launching additional supplies into space, NASA seeks to develop materials that can effectively perform multiple purposes. Therefore, one would like to design materials that can be used for both radiation shielding and another purpose, such as structural components (good mechanical properties) or thermal shields.

Currently, NASA uses aluminum for radiation shielding (4). This material is marginally effective at radiation shielding, since it has a low electron density. Therefore, researchers have been looking for other materials, which have higher hydrogen content than aluminum, to use as radiation shielding materials. Polymers have been a natural

area of interest, due to the possibility of creating very good multi-functional materials. Polyethylene is often used along with aluminum as a benchmark for making comparisons about the radiation shielding effectiveness of a new material. Polyethylene is of particular interest because it inherently has the highest hydrogen content possible in a polymer. Furthermore, polyethylene does not contain any large nuclei, which is important because the absence of large nuclei dramatically reduces the risk of the shielding material fragmenting from a collision with a radiation ion. That is beneficial, because it reduces the number of particles that must be dealt with by an effective radiation shield (5). Unfortunately, polyethylene does not possess particularly good thermal and mechanical properties, and so it is difficult to use it in the harsh space environment.

The purpose of this research is to use computer simulations of materials in the space radiation environment to determine how effectively they shield against radiation. Computer simulations are particularly important for evaluating the radiation shielding properties of materials, since it is extremely expensive to launch materials into space for actual experimentation. Furthermore, it is extremely difficult to develop an earth-based laboratory for this type of experiment. Therefore, it is of critical importance for manned space flight that there are accurate computer simulations to evaluate materials radiation shielding properties.

Physical Interactions between the Projectile and Materials (6)

In order to accomplish the goals of this research, there are several different types of computer codes that can be used. These codes fall into two very broad categories. First, there are deterministic codes, which use many assumptions and a mathematical approach to model the problem. These codes have the advantage that they can run in a relatively short amount of time. Included in this type of code are the NASA-Langley transport codes, GRNTRN and HZETRN. HZETRN is used for modeling the space radiation environment, while GRNTRN is used for modeling experiments to make comparisons about the accuracy of these deterministic codes. The next broad category is Monte Carlo codes. Monte Carlo codes make fewer assumptions, because they include more details about the physical interactions than deterministic codes, which run faster. This means that the code must run many times before the results are meaningful. The assumption in this type of code is that the average of all the results from running the code many times is the correct answer. Monte Carlo codes include many different codes, but this project chose to use GEANT4, which is capable of simulating the passage of particles through matter. However, all of these codes share the same goal that they are used to model the interaction between radiation and shielding materials.

All of these different types of code must somehow model what happens to particles as they pass through matter. Any time that there is a change in any property of the particle there is an interaction. These interactions are often referred to as physical interactions. There are numerous different physical interactions that GEANT4,

HZETRN, or any other code simulating radiation damage must be able to handle in order to model accurately the passage of particles through matter. This paper will explain the major processes that this project's GEANT4 based code considers. However, almost all of these processes are also used in HZETRN.

One extremely important physical interaction is Rutherford scattering. This phenomenon was famously exemplified by the Rutherford gold foil experiment. Basically, this occurs when the nucleus of a radiation particle passes close to a nucleus in the shielding material. There is a very strong electrostatic repulsion in this type of elastic collision, which causes a deflection of the radiation particle. This is relatively rare, because the chance of an energetic incident ion coming close enough to a nucleus to undergo a large deflection is very small. However, this process does occur with some frequency.

Even less likely than Rutherford scattering is the process of nuclear fragmentation. This is very similar to Rutherford scattering, except an extremely energetic projectile nucleus collides with a nucleus in the material with such force that one or both of the nuclei shatter forming at least two smaller nuclei. This physical interaction is what can cause ionic secondary particles in this project's simulation. This process is very important, because some of the heavy ions in the GCR spectrum have sufficient energy for extensive fragmentation to occur.

Another related interaction to Rutherford scattering is multiple scattering. In multiple scattering, there can be a large deflection of the incident ion, but it does not occur as the result of a single major coulombic interaction with another nucleus. Instead, multiple scattering occurs from multiple weaker interactions with several nuclei that the

ion passes near. This process is extremely important, because the likelihood of having one single massive collision with a nucleus is not as likely as the possibility of an ion passing near other nuclei and the combined effect leading to a large deflection.

There can also be energy loss through ionization. Ionization occurs when the charged radiation particle collides with an electron associated with an atom in the shielding material and the electron can be excited or even removed from the atom. If the atom is ionized, this is the equivalent of producing a secondary electron, since that electron is now free to travel through the shielding material causing further damage.

Furthermore, these free electrons can cause other damage from two types of processes. First, they can further ionize other atoms (or maybe just excite another electron in that atom) by colliding with another electron. This process is fairly similar to ionization by the collision of an ion with an electron. The other major process is bremsstrahlung. In bremsstrahlung, electromagnetic radiation is formed by the sharp acceleration of a charged particle, such as an electron, when it interacts with an atomic nucleus or another electron. Bremsstrahlung is far more important when considering electrons than it is for nuclei, because electrons have a far smaller mass than nuclei and so it is easier for them to experience the accelerations necessary for this process to occur.

Also, accelerating electrons radiate energy. This radiation is trivial compared to ionization for almost all electrons. However, for a few very fast moving electrons, this type of energy loss becomes the dominant one. Therefore, it is important to include this model into the physical interactions included in this project's code.

So far, this discussion has only considered nuclei and electrons. However, there has been a reference to processes such as bremsstrahlung producing electromagnetic

radiation. In addition, other interactions such as the decay of unstable particles can produce electromagnetic radiation. Therefore, it is also important to include models for the passage of electromagnetic radiation through matter.

There are several major interactions between electromagnetic radiation and matter. First is the photoelectric effect. In the photoelectric effect, electromagnetic radiation is absorbed by an atom and is used to remove an electron from an inner shell of that atom. This process can result in the production of more electrons, which must be treated as previously described.

The photoelectric effect requires that the electrons be bound to the atom in question. However, not all electrons are bound. Therefore, it is possible to have scattering on free electrons. This type of interaction is modeled by Thomson, Rayleigh, and Compton scattering. Thomson scattering is best exemplified by a free electron in a beam of X-rays. The free electron will oscillate with the X-rays. However, while in this oscillatory motion, the electron will radiate scattered X-rays. These scattered X-rays are an example of Thomson scattering. More generally, Thomson scattering can occur when any type of electromagnetic radiation is scattered by any charged particle. Rayleigh scattering is similar to Thomson scattering, except that it considers the scattering by all electrons present, when the momentum transferred by the photon is small compared to the momentum of the electron in an atom. In addition, Compton scattering is also very similar to Thomson scattering, except that it accounts for the shift in wavelength of the scattered radiation. Compton scattering must be used for very high energy photons, where the quantum properties of electromagnetic radiation become increasingly important.

The last important physical interaction that one must consider when electromagnetic radiation is involved is pair production. In pair production, a gamma ray is converted into an electron-positron pair. Pair production cannot occur in free space, because a nucleus or electron must be present to allow for conservation of energy and momentum in the transformation. Furthermore, the positron produced by pair production will be quickly annihilated by an electron. This annihilation will most commonly produce two gamma rays.

Lastly, one must consider the decay of a particle. This discussion about particle decay is very specific to GEANT, because there are many different approaches used to consider this problem.

First, many particles will decay with time. There are numerous particles that may be produced which are not stable over even the short periods of time being considered by this code. Therefore, GEANT4 must have a detailed method for accounting for the decay of these particles. Obviously, GEANT4 knows what type of particle it is tracking and whether or not that particular particle is stable. If decay processes are active, then GEANT will select the proper model of decay for the given type of particle (10).

The most common decay calculation method is a phase space decay. These phase space decays are simulated with isotropic angular distributions in the center of mass system. This decay process handles such common situations as the pion and delta particle decay (10).

Another common decay calculation method considered in GEANT is the Dalitz decay and some very related decay processes. The Dalitz decay process handles any decay where a spin-0 meson decays into a gamma and a lepton. GEANT handles these

processes by working with the assumption that the angular distribution of the gamma particle is isotropic in the center of mass system of the parent particle (10).

Muon decay is handled by applying the Fermi V-A Theory. This theory fairly accurately considers muon decay except that it does not predict the daughter neutrinos momenta. However, GEANT4 simply assigns them momenta isotropically in the center-of-mass frame so that energy is conserved in the decay process. For almost any case, this is an adequate assumption and it is certainly adequate for modeling space radiation, in which case one must worry much more about the heavy positive ions causing damage (10).

This has been a brief qualitative description of the major physical interactions that GEANT incorporates into the code. For a more detailed explanation of all of these processes Segré's book Nuclei and Particles is an excellent reference.

GRNTRN and HZETRN [(7) and (8)]

There are several different types of codes, which the radiation-shielding group at NASA-Langley have developed, in order to evaluate the shielding properties of different materials. Within the Langley codes, there are two very distinct types of codes that have been developed. First, there is a lab code, which is capable of mimicking experimental setups, and simulates a beam of one type of particle with a very narrow energy distribution passing through shielding material (8). The other type is the space code, which simulates the actual space radiation environment, including all the different types of particles at their correct energy distribution (8).

GRNTRN is the current generation lab code, which is named for the Green's functions that it uses. GRNTRN takes one type of projectile at one energy and impacts it with the shielding material. The shielding material can currently only have one layer. Unfortunately, it is not yet possible to simulate a shielding material with multiple layers stacked on top of each other by using GRNTRN (8).

The most important output from the lab code is the energy deposited graph. Energy deposited refers to the amount of energy deposited in the silicon detectors by whatever particles come out the backside of the target. These particles can be primary, which are the same particles that were accelerated down the beam line, or they can be secondary, which are particles that were produced during physical interactions with the shielding material. The energy deposited is crucial information, because it is the closest data to the raw experimental data, which is recorded at a nuclear accelerator facility. Therefore, one can use the energy deposited graphs to make comparisons with experiment in an attempt to validate the math, physics, and code. Eventually, the math

and physics in the lab code will form the next generation space code, which takes an actual spectrum of particles at realistic space energies. The space code simulates the space radiation environment as closely as possible. However, at the moment, the space code relies on HZETRN, which is an older model and more limited than GRNTRN.

Results of the Lab Code (8)

As mentioned earlier, the lab code takes one type of projectile particle at one specific energy and impacts it on a target or shielding material. There can be a very small spread in the energy of the projectile to more closely imitate the experiments. It has also been configured to mimic the experimental setup by attenuating through the detectors, which would be present in the experimental setup. This is needed, because there are detectors and triggers, which the particles must pass through before hitting the shielding material in any experiment. This, however, does not constitute a multiple layer code, because it does not allow nuclear fragmentation to occur in any of the detectors or trigger. This is a valid assumption, because the experimentalists will run a "target out run," which is essentially a background scan of the setup with everything except the target present. They can then subtract out any fragmentation that occurs in the detectors or trigger. Therefore, the experiment only measures the nuclear fragmentation in the actual target or shielding material.

The materials that were simulated by the lab code are polymeric materials that Brookhaven National Laboratory has tested. Unfortunately, Brookhaven did not send complete data sets and so it is more difficult to make comparisons with GRNTRN, since Brookhaven mostly provided analyzed data instead of raw data.

UDABDA1 ($C_{58}H_{42}O_8N_2$) was tested at Brookhaven with a 1 GeV/nucleon iron-56 projectile. Experimental values were recorded for the fluence of each type of charged particle. This can be compared to the numerical fluences predicted by GRNTRN, assuming they are both normalized to the same value. The experimental data and the numerical code predictions must be normalized to one, because the lab code does not predict how many iron-56 nuclei come off the beam line at Brookhaven in the variable amount of time that the experimentalists take to run the experiment. This comparison of the fluence for each type of particle is shown in Figure 2. Fluence is the number of particles to cross the detector during the experiment.

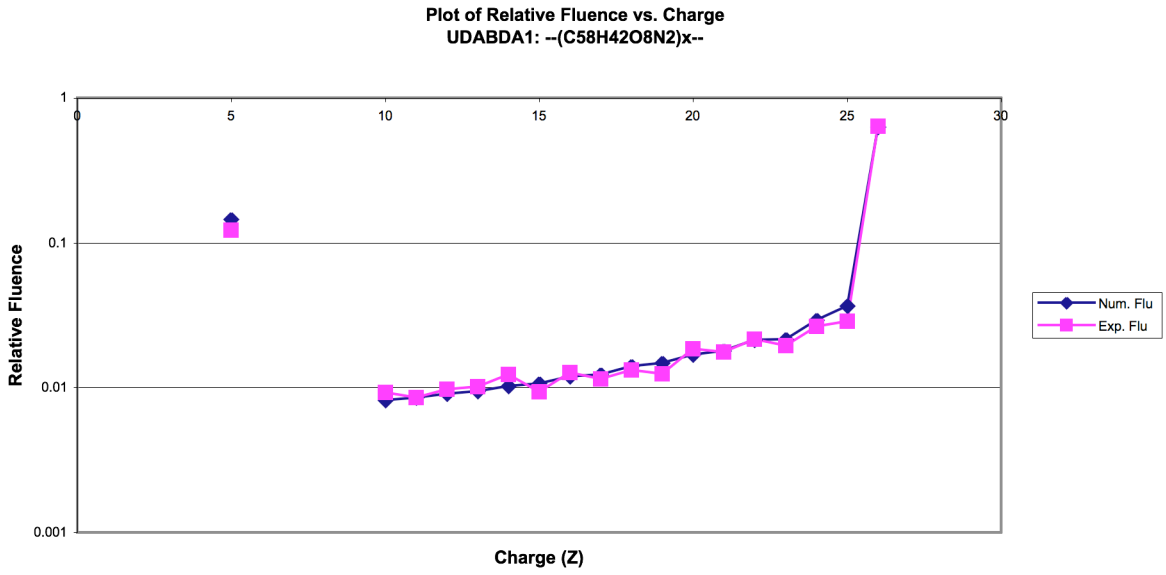

Figure 2. Comparison of Experimental Fluence with GRNTRN's numerical Fluence for each type of relevant particle.

Figure 2 shows very good agreement between theory and experiment. Agreement is nearly perfect for higher charge particles. The calculations, however, lack some of the dramatic odd-even effects, which the experiment clearly shows. This is a known deficiency in NUCFRAG, which generates the nuclear interaction cross sections used in

GRNTRN. Furthermore, all of the particles of charge 1 to 9 are grouped into a single data point. This is done because the experimental near detectors, which are the closest detectors to the shielding material and were used to measure this data, have very low resolution for low charge particles. Therefore, Brookhaven simply reported all of these particles with one single data point at a nuclear charge of 5. The numerical prediction from the code for fluence of particles at this single data point was the sum of the fluences for all particles having a nuclear charge of 1 to 9. The value is reported as having a nuclear charge of 5, since that is the midpoint. However, GRNTRN does slightly over-predict the fluence of these low charge particles, which is another known deficiency in the code. However, overall GRNTRN performs very well at predicting what will happen when a 1 GeV/nucleon iron-56 nucleus is bombarded against a UDABDA1 shielding target. This is an important observation, because it validates much of the fundamental physics and math in the code. Therefore, other predictions from GRNTRN are likely to be fairly accurate, since GRNTRN makes good predictions of what particles will be produced. This is the most fundamental output from GRNTRN, and is necessary to make all subsequent calculations.

Using the same shielding material, UDABDA1, with the same projectile of a 1 GeV/nucleon iron-56 ion, GRNTRN predicts the energy deposited in the silicon detectors used during the Brookhaven experiments as shown in figure 3.

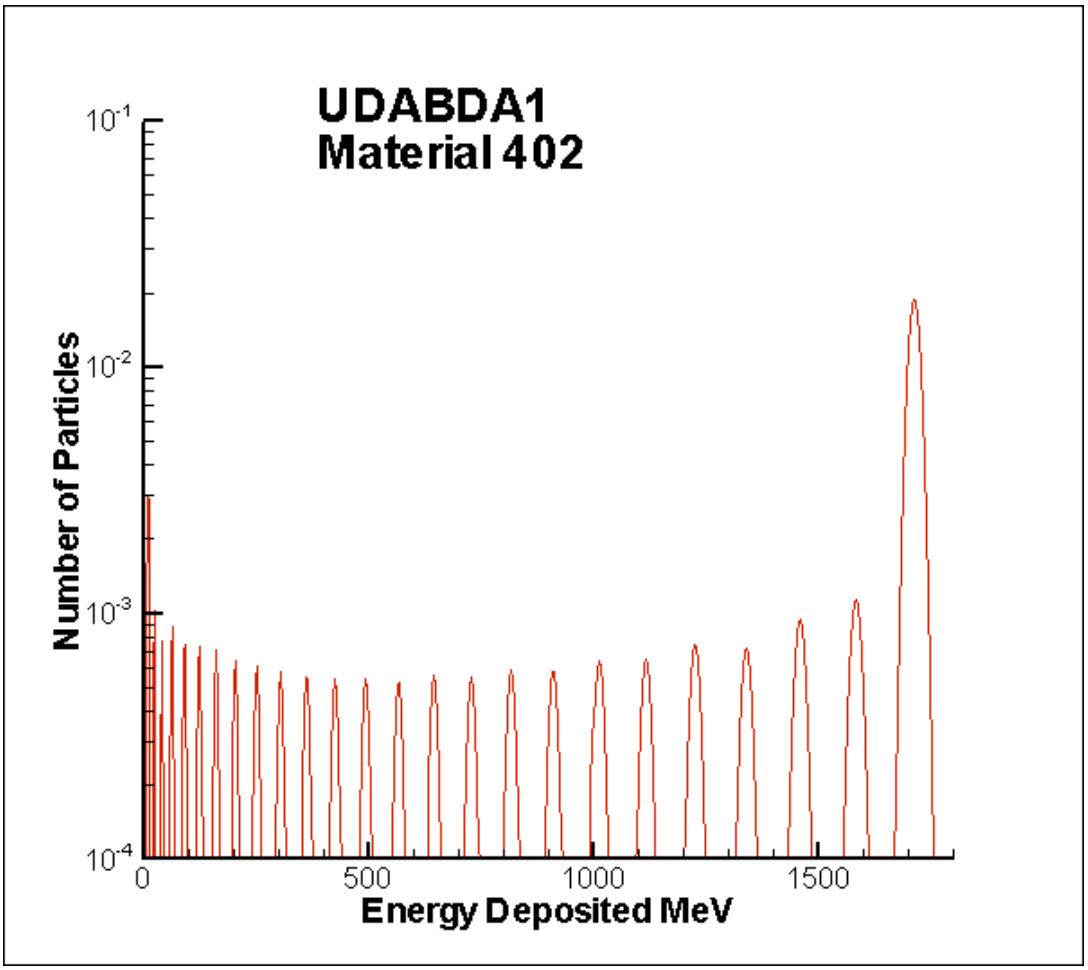

Figure 3. GRNTRN's prediction of the Relative Fluence vs. Energy Deposited in the Silicon Detectors used by Brookhaven.

Figure 3, produced using GRNTRN, contains some important information. The furthest right peak corresponds to the primary ion, which is iron (Z=26). The peak one to the left of the primary is manganese (Z=25). This pattern continues all the way to the leftmost peak, which is hydrogen (Z=1) (8). While the incident projectiles are iron-56 nuclei, they will fragment forming all possible smaller nuclei. These smaller nuclei as well as the iron nuclei will deposit a discrete amount of energy in the detectors based on their nuclear charge. Obviously, this is important because it tells the relative number of particles and predicts the amount of fragmentation, which is likely to occur.

Fragmentation occurs when the primary particle is split into multiple smaller, secondary particles. Secondly, figure 3 also shows, under close examination, some of the odd-even effects, which are a well understood phenomenon in nuclear physics (8). The odd-even effect is most visible with particles having a nuclear charge in the teens. Also, the graph shows that hydrogen and helium are produced at a much higher rate than other fragments. Furthermore, one can see why some fragmentation is good, since it must produce smaller particles, which deposit less energy in the internal environment of the spacecraft, consequently reducing the radiation dose that astronauts and electronics in the spacecraft receive. However, the problem with fragmentation is that it produces more particles and so it can be potentially more dangerous, since one increases the number of particles that interact with the internal spacecraft environment.

Despite the good fit between models and experiment that was shown by UDABDA1, there are still some technical problems associated with GRNTRN. One problem is a potential problem with the energy downshift formula. Energy downshift is the loss of energy associated with the process of nuclear fragmentation, since collisions between nuclei are not perfectly elastic. The energy downshift formula is a relatively simple model and was originally calibrated for iron projectiles. However, Brookhaven provided some experimental data, which they had measured using various metallic shielding materials and polyethylene with a silicon projectile, which is a common choice for radiation experiments, since silicon corresponds to a peak in the GCR spectrum.

The comparison between experiment and GRNTRN's model is shown in figure 4, which shows a graph of relative fluence versus energy deposited in silicon detectors.

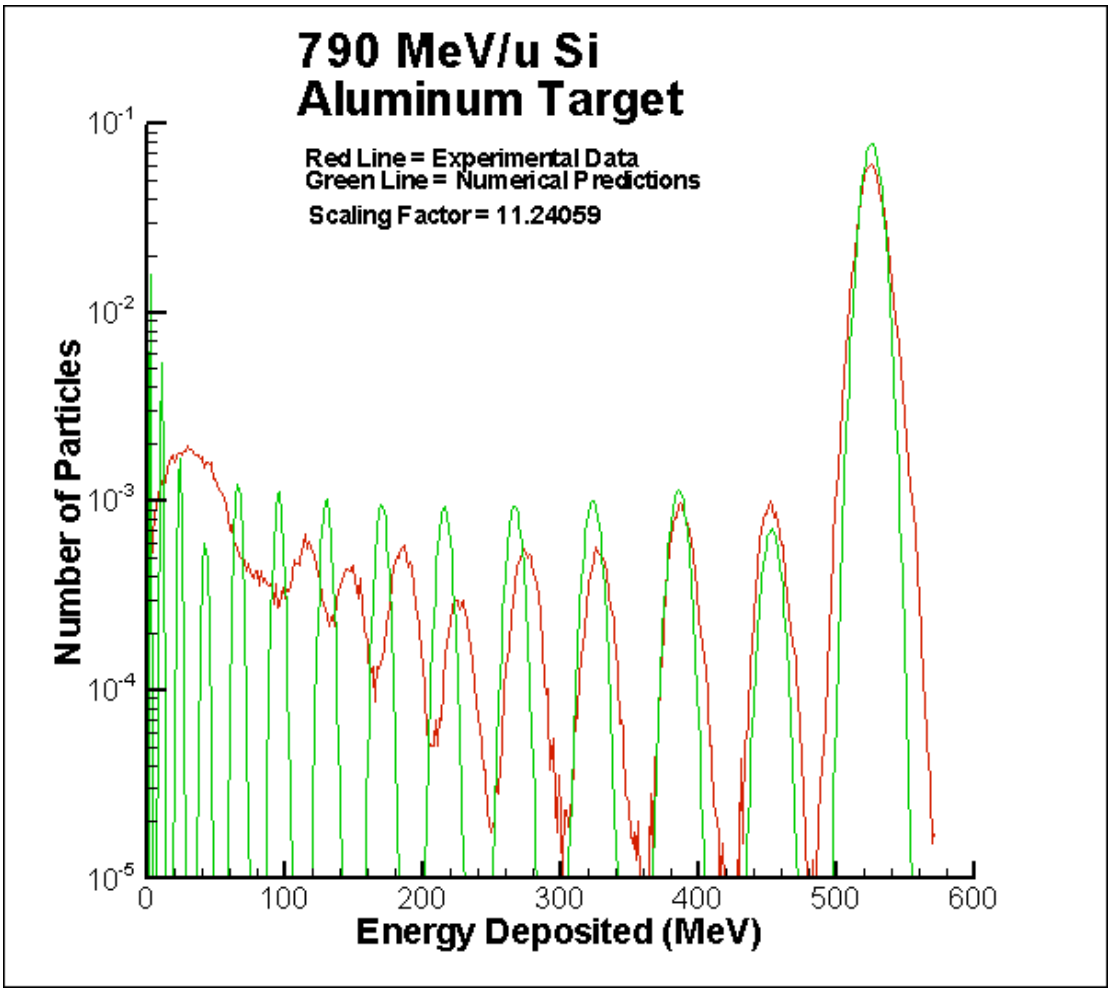

Figure 4. Comparison between Experimental data and GRNTRN using a plot of relative fluence versus energy deposited in silicon detectors at Brookhaven.

As one can see, this is only a decent match between theory and experiment. One is able to largely ignore the low charge particles, since the near detectors, which measured these experimental data, have very little resolution for low charges. However, it is very evident that the code predicts dramatically more fragments than were actually produced. This may be somewhat a problem of normalization, due to the lack of resolution at low charges, which makes it difficult to obtain an accurate total number of all particles, but that explanation probably does not account for all of the problems (8). However, more importantly, the code is showing significantly less interaction for the

mid-charged particles than Brookhaven measured. Less interaction between the projectile and shielding material corresponds to less energy being deposited. This is probably because the energy downshift formula is off. It may well be underestimating the energy loss for fragmentation, which will result in this graph. That situation would produce a graph like this, because the particle would be traveling through the shielding material at a higher energy, which would result in less interaction (mostly coulombic interactions between the electrons of the shielding material and the positive charge of the projectile ion). With less interaction between the projectile and shielding material, there will be less energy deposited in the detectors, which is exactly what this graph shows.

Further complicating the situation is the problem of coincidence. This is an experimental phenomenon, which occurs when two ions hit the detector at the same time (8). The detector does not know that there are two particles. Instead, it sees one particle with a charge of the square root of the sum of the squares of the two particles' charges. Therefore, coincidence could account for some of the discrepancy in the energy deposited, since that would raise the value of energy deposited above what it should be. Also, coincidence is relatively more likely for the near detectors than the far detectors, since the particles have less time to spread out, and so coincidence is less likely to occur in the far detectors. Unfortunately, Brookhaven did not provide the raw data from the far detectors and so it is impossible to ascertain how much of a problem coincidence was in this experiment.

Yet another complication in this comparison graph is that Brookhaven recorded the fluences as a function of linear energy transfer (LET), instead of energy deposited in the detector (8). LET is the amount of energy deposited per unit length in the material.

Therefore, to obtain the energy deposited, which is what GRNTRN predicts, the Brookhaven data was scaled linearly, because the experimentalists said that LET is linearly related to energy deposited. Unfortunately, since there are no data recording the energy deposited, it is impossible to see if the relationship is almost exactly linear or only approximately linear. The absence of an exact linear relationship could further explain the shift between where the experimental data and the numerical data fall on this graph. Clearly, there are still several possible explanations for the poor fit between experiment and theory shown here. Most likely, it is some combination of these different possibilities, which is causing the error. This is an area where further studies could be conducted to narrow the gaps between experiment and GRNTRN.

In conclusion on the lab code, this has been a brief description of some of the work that has been conducted using GRNTRN. Overall, GRNTRN is fairly consistent with experiment and probably quite accurate at predicting space radiation. Therefore, it will be a big advance, when GRNTRN is able to model the actual space radiation environment.

Results from the Space Code (7)

The space code is different from the lab code, since it uses many different types of projectiles at an actual distribution of energies as seen in space. This is obviously quite useful, because it enables one to model the space radiation environment using a computer simulation. The most common type of output from the space code is a dose depth curve. Dose depth curves plot dose equivalent versus depth in the shielding material. Dose equivalent is a biologically weighted measure of radiation dose. Furthermore, the dose depth curves are produced for both a GCR and SPE spectrum. The solar particle events

have many fewer heavy particles, which are more dangerous than lighter particles, but the shear number of particles in a SPE can make these events extraordinarily dangerous to manned space missions. The spectrum used for GCR in HZETRN is shown in figure 5, while the King Spectrum used for SPEs in HZETRN is shown in figure 6.

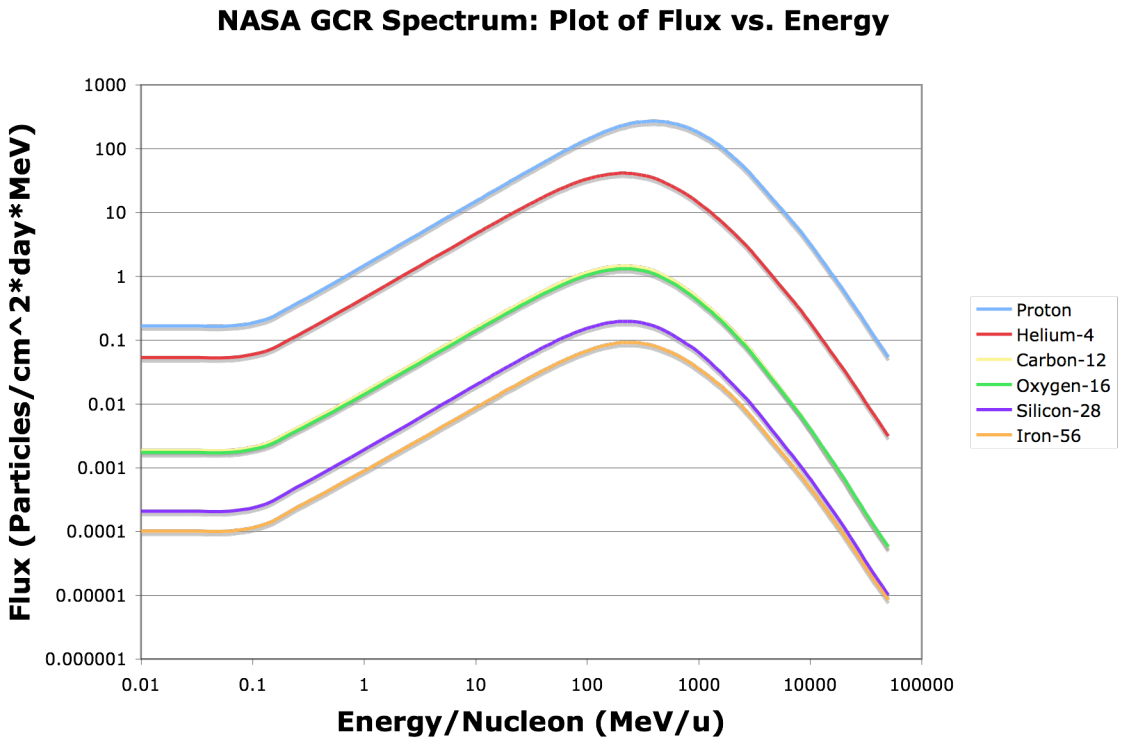

Figure 5. GCR Spectrum used in HZETRN showing the flux versus the energy per nucleon for the six major particles in the GCR spectrum.

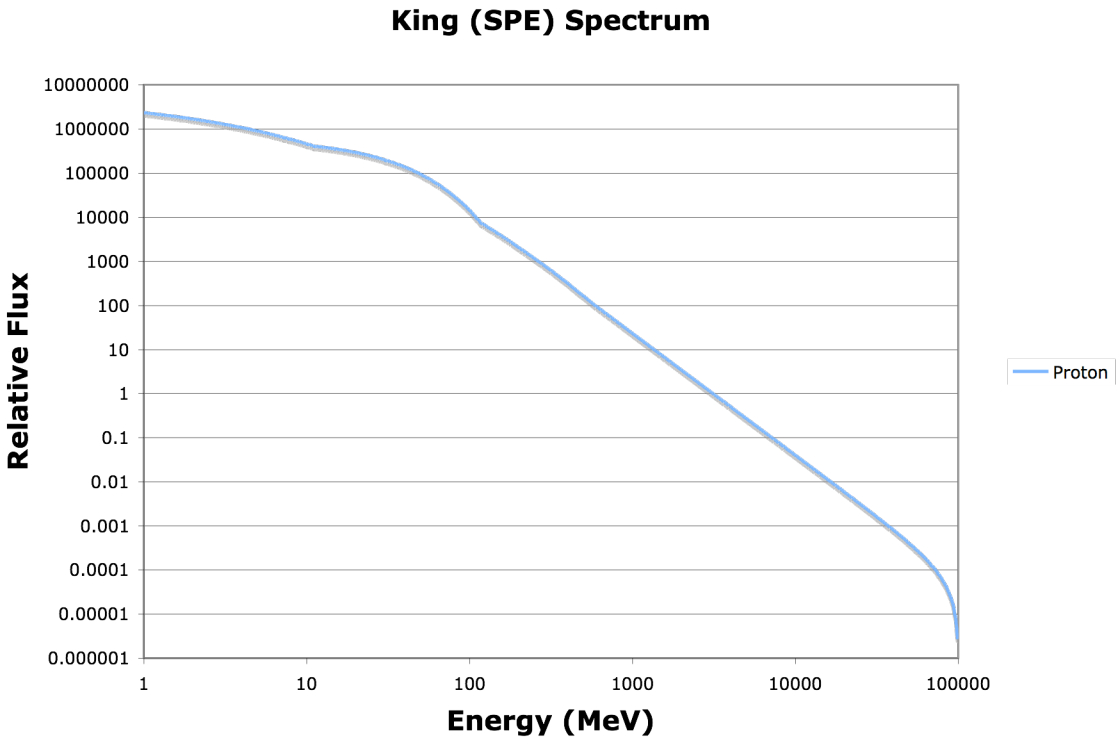

Figure 6. SPE Spectrum used in HZETRN showing the relative flux versus energy of protons in this SPE from August 1972. The total number of particles in this spectrum is normalized to $6.494*10^{11}$ protons/event.

In order to produce these data points, the space code uses the HZETRN transport code. This code is significantly older and less mathematically advanced than GRNTRN, which the lab code uses, but it is still fairly accurate for the very broad distribution of energies that the GCR and SPE spectra have. GRNTRN is more accurate, and it can deal with a spectrum of particles that has little or no spread in energy. GRNTRN makes its predictions using the Green's functions, whereas HZETRN uses many more mathematical approximations and assumptions (7).

Dose depth curves are very convenient plots, because they are some of the most easily understood. All that the curve shows is how much radiation exposure, which is the

dose equivalent, there is at a given depth with a certain shielding material. Therefore, if the dose equivalent (y-axis) is lower for one shielding material at a given depth than it is for another shielding material at the same depth, then the first material is a better radiation shield than the second material. So, the better shielding materials appear lower on the graph. This is useful, since it allows researchers to assess whether or not two different materials are significantly different from a radiation shielding point of view or not. Furthermore, since HZETRN simulates the actual space radiation environment, one can draw rather broad conclusions about the effectiveness of radiation shielding materials, whereas one must be far more careful with GRNTRN because that code only shows that a material is a better shield for one type of particle at one energy. However, that situation is not representative of space and can produce misleading results if one examines the shielding properties of materials using GRNTRN with an uncommon projectile at an uncommon energy. Therefore, one cannot say that GRNTRN will definitively identify the best shielding material.

Figure 7 is the calculated GCR dose depth curve for the polymeric materials that Brookhaven tested. It also includes polyethylene and aluminum since those have been two standard benchmarks for making comparisons about the effectiveness of radiation shielding materials. Polyethylene is considered a very good shield, since it has the highest hydrogen content possible in a polymer, whereas aluminum is not a good shielding material, due to its low electron density. To give some further understanding of this figure, the names of polymers with empirical formulas are listed in order from top to bottom: Aluminum (Al), Ultem ($C_{37}H_{24}N_2O_6$), Polysulfone ($C_{22}H_{27}O_4N$), PMDABDA1

($C_{37}H_{24}O_6N_2$), UDABDA1 ($C_{58}H_{42}O_8N_2$), UDABDA2 ($C_{62}H_{50}O_8N_2$), BPBPA ($C_{28}H_{22}O_3$), Noryl 731 (C_8H_8O), and Polyethylene (CH_2).

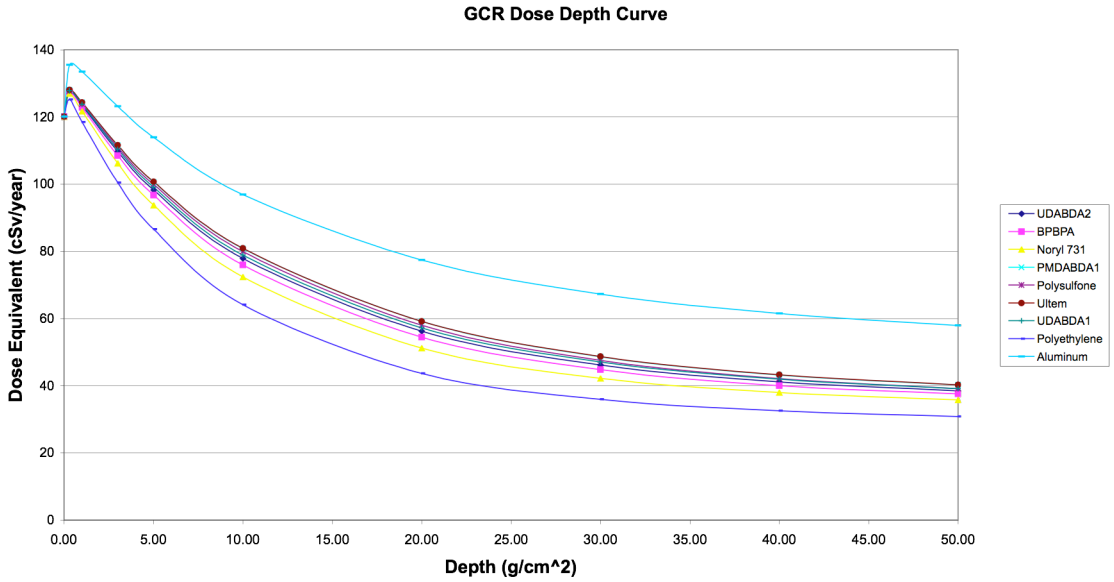

Figure 7. GCR Dose Depth Curve for various Polymeric Materials and Aluminum.

Figure 8 shows the same materials, which appear in the same order from top to bottom as figure 6, after being exposed to a SPE spectrum.

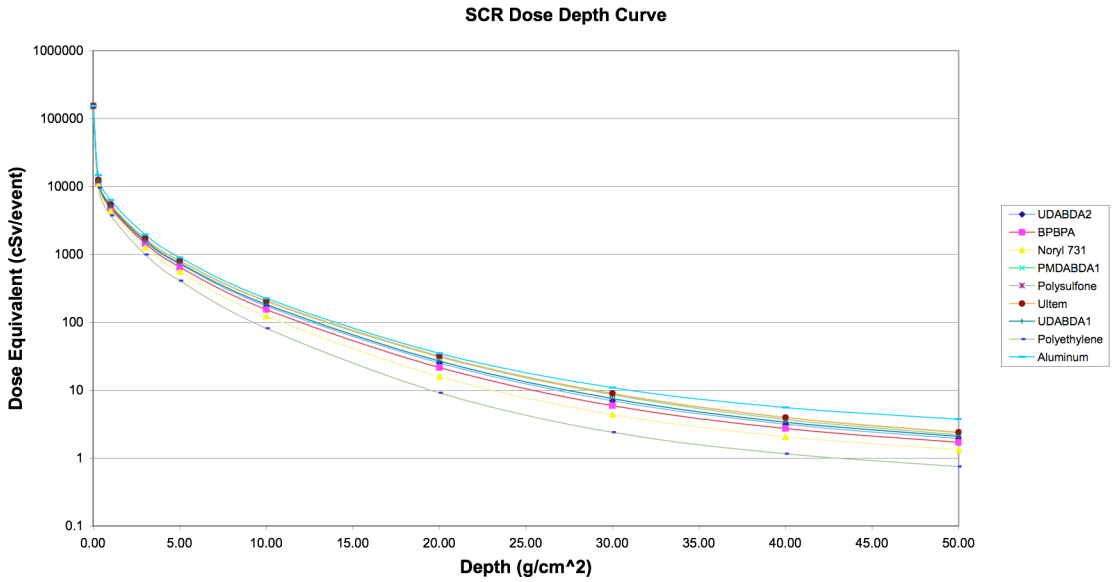

Figure 8. SPE Dose Depth Curve for various Polymeric Materials and Aluminum.

Figure 9 is a blowup of figure 8 in the region of 30 g/cm^2 depth.

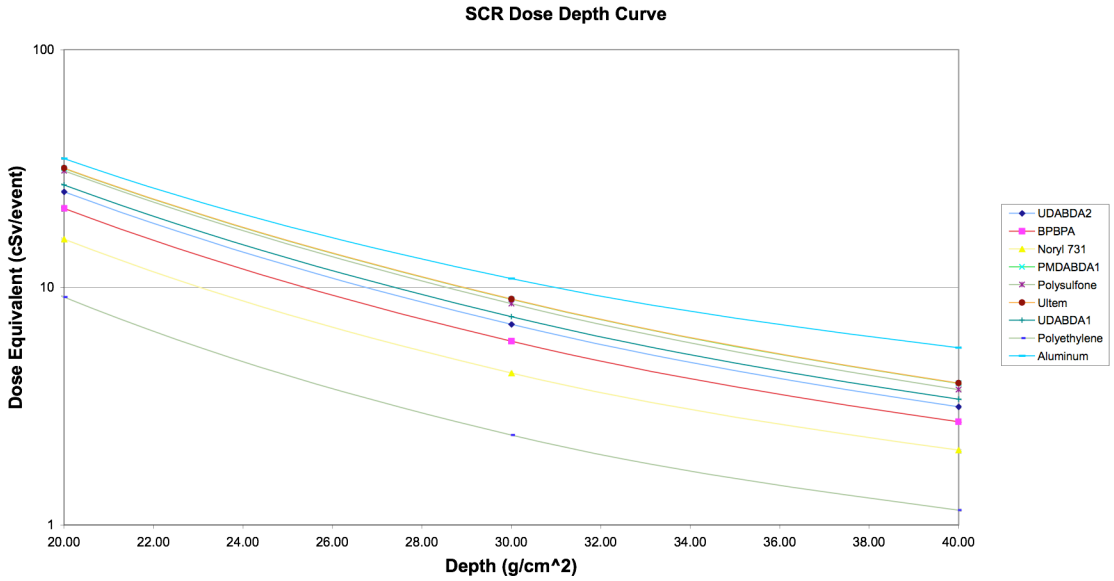

Figure 9. Blowup of SPE Dose Depth Curve for various Polymeric Materials and Aluminum around 30 g/cm^2 depth.

Clearly, Polyethylene is the best shielding material for both GCR and SPE. Aluminum is the worst shield in both cases. The second best shielding material for both the GCR and SPE spectra is Noryl 731, a commercial polymer. Noryl 731 is noticeably better than any of the other polymers. BPBPA is the next best shield for both GCR and SPE.

On the GCR graph, one can see that a little bit of shielding material (approximately 0.5 g/cm^2) actually increases the dose equivalent above the level of no shielding material. This is due to the nuclear fragmentation. Therefore, multiple particles must be dealt with instead of one, and so the result can be a more dangerous situation than if one had no shielding material. So, nuclear fragmentation is good, since it results in the formation of lighter particles, which are easier to slow and also since they are less damaging biologically; but it is bad, since there are more particles to slow after

fragmentation. This is a complicated set of tradeoffs to find the best shielding material with a thickness that adequately protects astronauts and equipment but can still actually be launched into space.

On the SPE dose depth curve, the dose equivalent falls off extremely fast as a function of depth (dose equivalent is plotted on a logarithmic scale). This demonstrates that SPE are almost entirely low energy protons, which are easier to shield against. However, the values of dose equivalent are still extremely high at low depths, since there are huge numbers of particles associated with the SPE. One needs approximately 10 g/cm^2 of shielding to reduce the dose equivalent down to the level of no shielding material for the GCR background. That shows the dangers associated with SPEs quite well.

It was already explained why liquid hydrogen is the best shielding material for dealing with radiation particles. Now, to show quantitatively how much better liquid hydrogen is compared to even polyethylene, a dose depth curve showing liquid hydrogen compared to polyethylene and aluminum for the GCR spectrum is shown in figure 10.

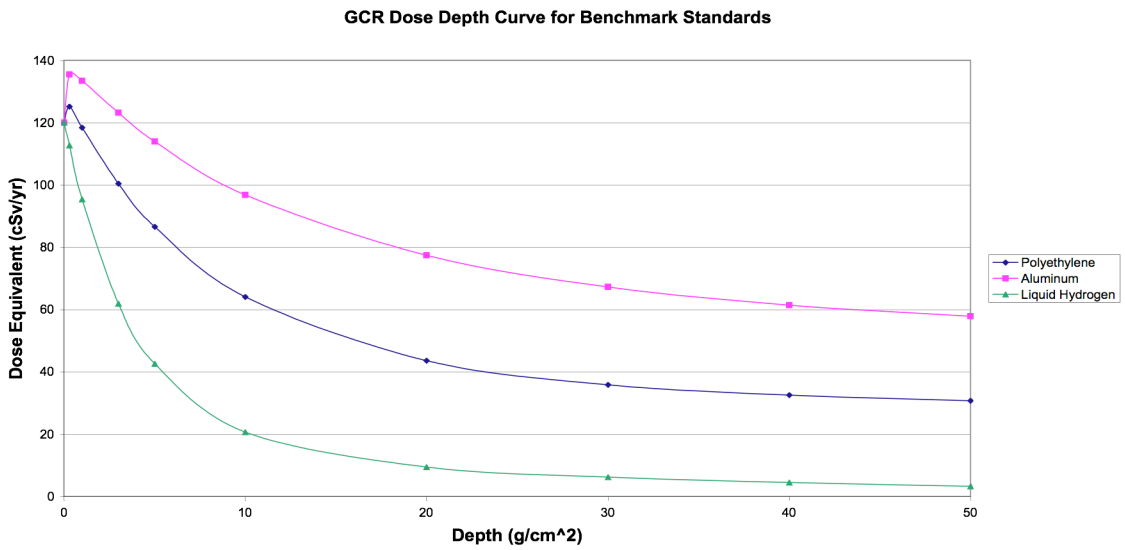

Figure 10. GCR Dose Depth Curve comparing Liquid Hydrogen to Aluminum and Polyethylene

Figure 11 shows the SPE dose depth curve for liquid hydrogen, polyethylene, and aluminum.

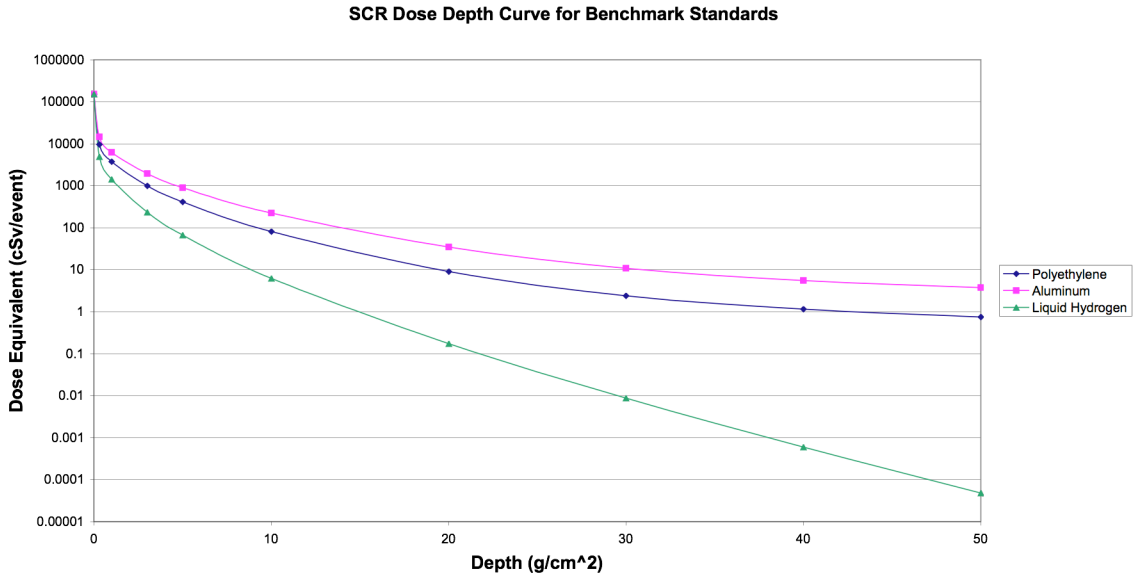

Figure 11. SPE Dose Depth Curve comparing Liquid Hydrogen to Aluminum and Polyethylene

Liquid hydrogen performs very much better than either aluminum or polyethylene for both GCR and SPE. In fact for SPE, by 50 g/cm^2 of liquid hydrogen, the dose equivalent value is at less than one ten-thousandth of one cSv/event, which is very little radiation exposure. (Centisieverts (cSv) are the units most typically used to measure dose equivalent and are dimensionally equal to centijoules per kilogram.) Similarly, for GCR, liquid hydrogen is very near 0 cSv/yr by 50 g/cm^2. These two graphs verify that liquid hydrogen really is the best radiation shielding material for space use. It also justifies why so much effort is being exerted to add more hydrogen content into polymer shielding materials.

Development of a Transport Code based on GEANT4

GEANT4 is a software package, which contains the tools necessary to model the passage of particles through matter (9). GEANT4 is capable of modeling any particle passing through any matter in any geometry (9). GEANT4 can be configured to control all aspects of the simulation from generation of the primary particles to recording the data being studied (9). At the core of GEANT, there is C++ code, which simulates a large number of physical models, which are capable of handling a wide energy range (9).

GEANT4 was developed in its current form by CERN, a nuclear accelerator in Switzerland, in 1993. This transition in 1993 made GEANT4 far more functional for a large range of simulations than its predecessor GEANT3 was.

GEANT4 is a Monte Carlo code. That means that the code generates one primary incident particle and transports that particle through the user-defined geometry. GEANT4 tracks all of the interactions that that single primary particle has. It then records all of the data that the user has specified to be recorded. Next, GEANT repeats the process all over again. GEANT will continue repeating the same setup until the user specifies that sufficient statistics have been achieved. Therefore, there can in theory be very few assumptions, either mathematical or physical, being made. However, one must run the code many times before the statistics of the data are adequate. This shows that Monte Carlo codes have an advantage over deterministic codes, because they can make fewer assumptions, but they have the huge disadvantage that it takes far longer to run the code before the statistics are adequate to provide strong results. In this project, this disadvantage becomes especially problematic for the GCR spectrum at large depths of shielding material. The heavy ions in the GCR spectrum, such as iron-56, have a high

frequency of fragmentation as they pass through the shielding material. However, there are so many different possibilities for the products of the fragmentation of a heavy ion, that it takes a huge number of primary particles before there are sufficiently good statistics for any given individual fragmentation process. Therefore, one sometimes has to input a tremendously large number of primary particles while using GEANT4. This is very different from HZETRN and GRNTRN, which have taken all of these different processes into account with their mathematical approach to the problem. Therefore, HZETRN and GRNTRN are capable of producing data in far less time than GEANT.

A major goal of this research was to develop a code, which could be used to make comparisons with HZETRN using GEANT4. The goal is to duplicate HZETRN's results using GEANT. This would provide a huge amount of confidence in HZETRN, which is difficult to experimentally verify, if GEANT produced very similar results. GEANT and HZETRN work in such inherently different ways that it is very unlikely that they are both wrong in the same way. Therefore, similar results would strongly imply that both codes are probably quite accurate.

This research did produce a code, which is capable of replicating the trends that HZETRN predicts for SPE. Unfortunately, due to time constraints, the code based on GEANT has not been developed to the extent necessary to compare directly with HZETRN for most materials. The main output from HZETRN predicts dose equivalent, which is a derived radiation unit that provides a biological weighting of the risk of the specific type of radiation. However, it is more difficult to calculate the quality factor necessary to scale dose into dose equivalent. Therefore, the code using GEANT currently is only capable of producing results in terms of dose. Hopefully, another later

project may continue work on this code and provide a more direct comparison with HZETRN by upgrading the code to include the ability to calculate the quality factor and dose equivalent. Also, a huge limitation of this GEANT based code is that it is only capable of effectively handling SPEs. The GCR spectrum, which contains many heavier ions, requires a more sophisticated handling of fragmentation, which has not yet been developed in this GEANT4 code to the extent necessary for handling GCR. Therefore, this GEANT code is currently only capable of accurately modeling SPEs, but this is an area for another future project to expand the capabilities of this code.

The code based on GEANT has the following geometry configuration as shown in figure 12. First, the incident beam is generated along the x-axis. This beam can be of a single energy or of an energy distribution. However, the beam of primary particles can only be of a single type of particle. Therefore, to generate a spectrum with many different ions in it, the code must be run multiple times with a different particle beam until all the major ions in the spectrum have been included. This is not at all a limitation for SPEs, since those consist almost entirely of protons. All other ions are so uncommon, that it is safe to ignore them. Furthermore, for making comparisons against HZETRN, HZETRN only considers protons in SPEs (7). However, it is not as clear cut an issue with GCR, since the GCR spectrum includes many more ions, and so the user must determine which ions to include and which not to include, whereas HZETRN even includes many uncommon isotopes.

After the primary particles are generated and traveling along the x-axis with their specified energy distribution, they will impact the shielding material. The user can specify any type of material as the shielding material. Furthermore, the user can specify

the thickness of the shielding material. The particles will pass through the material and any interactions that occur are recorded. Furthermore, all the particles will be tracked including fragmented particles from both the primary particle (or even a secondary particle from a secondary particle of the primary ion) and the shielding material. This is another similarity between HZETRN and GEANT. However, GRNTRN does not consider and track particles that occur from fragmenting nuclei within the shielding material (8). These particles interact with the shielding material until they either are stopped in the shielding material or they pass completely through it. Those particles that do not stop in the shielding material pass through it into water. The water is 1 g/cm^2 or 1 cm deep. Those particles will also continue to interact with the water until they are either stopped or pass completely through it. However, the radiation dose in the water is what is of interest. This dose is taken in water, because water can be used as a crude approximation of a biological system such as an astronaut, since all living cells are mostly water. 1 cm of thickness for the water was chosen after consultation with Dr. Steve Blattnig at NASA-Langley (7). He believed that 1 cm of water would make the best comparison to make with HZETRN, which also measures the radiation dose in water.

After the particles pass through the water, GEANT no longer continues to track them. This is because there is nothing of interest for this project with what happens to the particles after the water, and to continue tracking those particles would dramatically increase the time that it takes to run the code.

Again, the experimental setup of the code can be visualized as shown in figure 12.

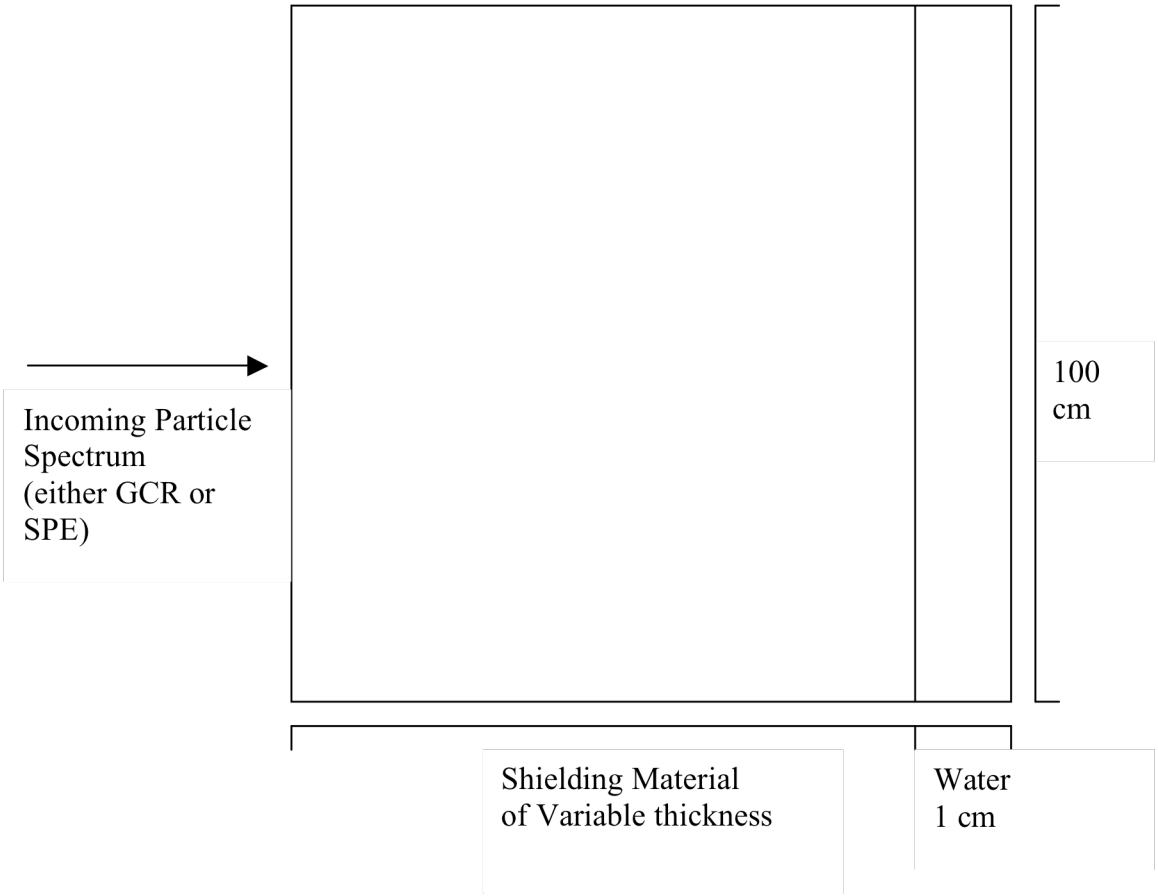

Figure 12. Visualization of the geometry used in GEANT4.

After the primary particles are generated with the correct energy distribution for the SPE or GCR, the code runs many times. The SPE Spectrum used is the King Spectrum from August 1972 and the GCR spectrum is the default GEANT4 GCR spectrum.

After a sufficient number of primary particles have been generated, GEANT will record how much energy is deposited by each particle in the water. Many of the primary particles will not deposit any energy in the water, because the low energy particles do not have enough energy to make it through a relatively thick shielding material. Therefore,

these particles never reach the water and cannot deposit any energy. This project has chosen to record the remaining data using Root, which is a data analysis framework created by CERN, which also made GEANT4. Root is capable of recording many different data points and recording them into an easily accessed file. One small downside is that one must use binning with Root. Root works by filling histograms and so there is not infinite resolution of the data recorded in Root, since one must decide how many bins to use to record all the data points. This is a small problem, since one wants to create small bins to maintain accuracy, but by increasing the number of bins one will further slow down the program. Therefore, one must again make a compromise between speed of the code and its accuracy. However, if one generates a sufficiently large number of primary particles, the loss of accuracy of the recorded data should average out with a large number of events in each bin. Then, Root can analyze the data and produce the average energy deposited in the water by a single primary particle. This is the most important data output from this project's code. To obtain this data point, the code used between 10,000 and 30,000 primary protons in the King (SPE) Spectrum. There were a huge number of primary ions used for the SPE spectrum, because SPEs have far more particles at very low energies. These particles interact more with the shielding material and the water and so there is a greater possible variation in the outcome. Therefore, one had to use far more primary ions to reproduce the results. The test for checking whether a sufficient number of primary particles was used was to choose one material and see if the data points for polyethylene could be reproduced to within 5%. This is often referred to as a convergence test. While this may seem like a relatively large difference, this was the compromise chosen in order to have the code run in a reasonable amount of time. For

GCR, there were 1,000 primary ions of protons, helium, carbon, oxygen, silicon, and iron used, most of which had significantly higher energy than the SPE protons. There was good convergence using this number of primary particles, which include the six major ions in the GCR spectrum. After consultation with Steve Blattnig, it was decided that it was sufficient to consider only the six major components of GCR (7).

After Root recorded the average energy deposited by one type of particle with an appropriate energy distribution, the data could be analyzed. One had to know the total number of each type of particle. This information was provided by Dr. Steve Blattnig. The King Spectrum for a SPE consisted of $6.494*10^{11}$ protons/event*cm^2. With this information, one can calculate the total energy deposited by the King Spectrum. This relies on the assumption that none of the particles will cross paths in either the shielding material or the water. This is a fairly reasonable assumption, since it is relatively rare for a particle to have a dramatic change in direction after an interaction in the material, although some of the nuclear collisions can produce that result. However, the nuclear collisions are far less common than the coulombic interactions between the projectile and the electrons in the material, which do not cause dramatic changes in direction, and so this assumption is valid. The GCR spectrum contains 537,305 protons/cm^2*day, 192,755 helium nuclei/cm^2*day, 18,261 carbon nuclei/cm^2*day, 22,281 oxygen nuclei/cm^2*day, 5,979 silicon nuclei/cm^2*day, and 6,576 iron nuclei/cm^2*day (7).

Then, the total energy deposited by the incident spectrum can be converted into radiation dose by dividing the total energy deposited by the mass of the water. One will notice that the total number of particles is dependent on the cross-sectional area of the shielding material. However, the mass of the water is also dependent on the exact same

cross-sectional area, since the water was chosen to have the same cross-sectional area as the shielding material. Therefore, this area dependence will cancel out when calculating radiation dose. Furthermore, one typically expresses radiation dose in units of Grays. 1 Gray is equal to 1 J/kg. Therefore, one can see how easy it is to convert from energy deposited into dose by a simple division.

Using this computational setup, one is able to produce dose depth curves similar to HZETRN by using GEANT. The major difference between these curves and those already presented that were made using HZETRN is that this GEANT based code calculates dose as opposed to dose equivalent, which HZETRN calculates. This would be a possible future project where this GEANT based code could be more directly compared to HZETRN, by calculating the quality factor and converting dose into dose equivalent. However, these graphs should have the same shape and order of shielding material for an SPE, because dose equivalent is derived from the dose and there is almost no fragmentation in an SPE, which can dramatically change the quality factor. Dose equivalent is the biological measure of radiation damage and multiplies the dose by a quality factor, which attempts to weight the biological damage from different types of radiation. However, they are dimensionally the same, because the quality factor is dimensionless. Therefore, 1 J/kg is equal to both 1 Gray and 1 Sievert, which is the standard unit used for dose equivalent. This shows why these graphs should have the same shape and relative order of shielding materials as HZETRN does for SPE. Unfortunately, this similarity does not hold true for GCR, since the GCR spectrum includes fragmentation where a heavy nuclei forms multiple smaller ones. Therefore, the quality factor immediately goes from a large number to a much smaller one with

fragmentation. This shows why the dose equivalent falls off rapidly for GCR. However, the dose from GCR does not fall off rapidly. Instead it should rise above the value for no shielding material, due to fragmentation, and then only slowly fall off from that maximum value.

Using this procedure for the GEANT based code, the dose depth curve was produced for the King Spectrum, which was a SPE in August of 1972. This is the same spectrum that HZETRN used and is shown in figure 6. These results are presented in figure 13.

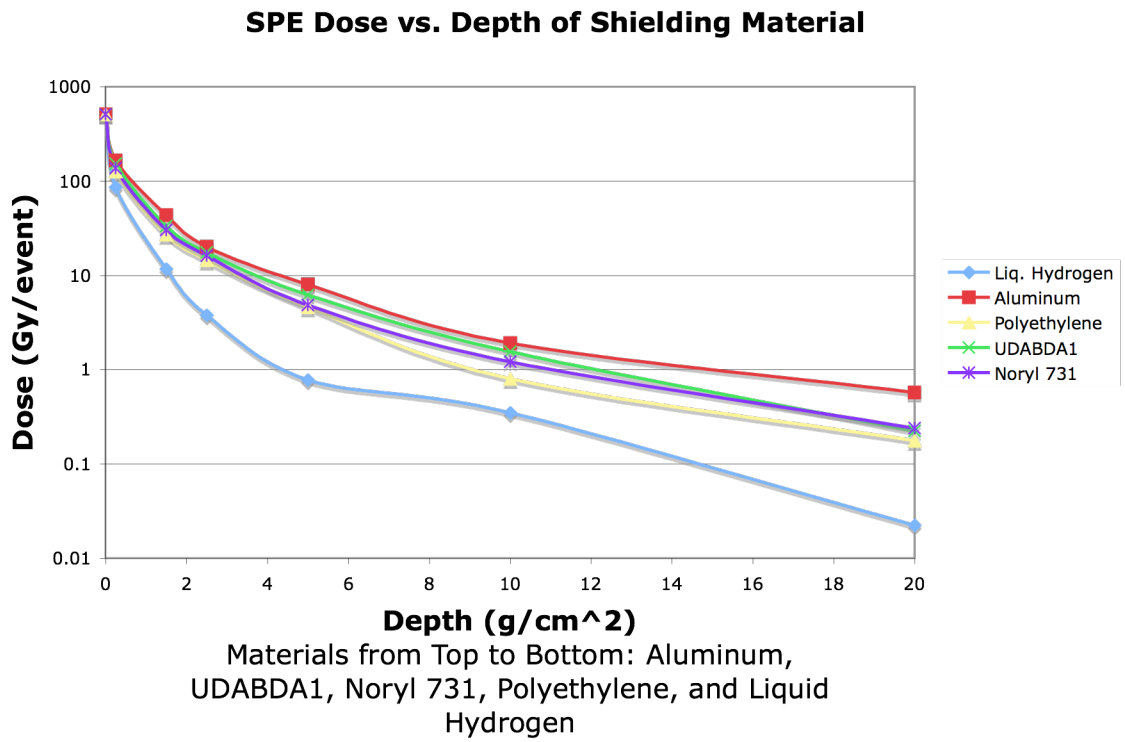

Figure 13. SPE Dose Depth Curve for various Materials using the GEANT4 code.

Figure 13 shows the same general shape and order of materials as HZETRN does. It also confirms that SPEs are relatively easier to protect from since the dose falls off so rapidly. However, the SPE particles are incredibly dangerous, because they start from

such a massive level of dose. With no shielding, it would be impossible for a human to have survived being in deep space with the King Spectrum occurring. It is also important to note that this graph is also good confirmation of HZETRN, because it also replicates the same rank order of shielding materials as well as the same shape as HZETRN's dose depth curve.

To show a direct comparison to the dose prediction by HZETRN, there is a comparison of the dose for aluminum using both GEANT4 and HZETRN. This comparison is shown in figure 14. Figure 14 shows that the results from GEANT4 are capable of replicating the correct shape of the results. However, the GEANT code is overpredicting the dose at large depths for this GCR spectrum. This becomes a significant difference at large depths. However, this may be a problem with the thickness of the water, in which the dose is being deposited. These GEANT results are the dose in 1 cm thick water. However, 1 cm of water may not be equivalent to what is used in HZETRN. 1 cm was chosen after consultation with Dr. Steve Blattnig, who thought that 1 cm would be fairly comparable. Changing the thickness of the water would shift the graph up or down. Therefore, this is an area for a future project, where another student could determine the ideal thickness of water for replicating HZETRN's results. However, the important feature of this comparison is that the shape is correct, which means that it is mostly a matter of fine-tuning the program to obtain a very good comparison between GEANT and HZETRN.

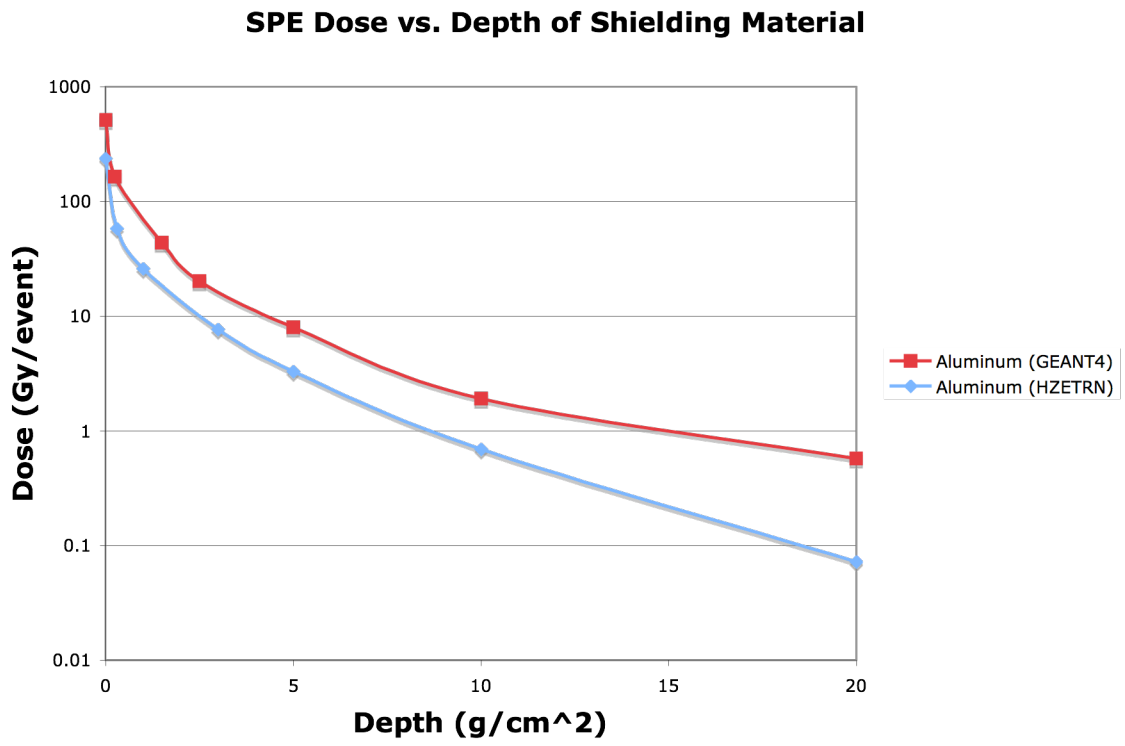

Figure 14. Comparison of GEANT4 and HZETRN Dose Depth Curves for Aluminum.

Unfortunately, the same level of accuracy was not achieved for the GCR spectrum. The GCR spectrum has many heavy ions in it, which have a high frequency of fragmenting. This frequent fragmentation leads to a huge number of secondary particles that continue to deposit energy in the water. This means that the dose does not fall off very quickly for the GCR spectrum. However, using this GEANT based code, the dose fell off approximately exponentially. This should not be the case due to the fragmentation. Therefore, that suggests that the GEANT code is not treating fragmentation correctly. However, after these results were already produced, it was also discovered that the default GCR spectrum included with GEANT4 is actually quite

different in appearance from the GCR spectrum that HZETRN uses. This can be seen by looking at figure 15, which shows the GCR spectrum used for the GEANT4 based code.

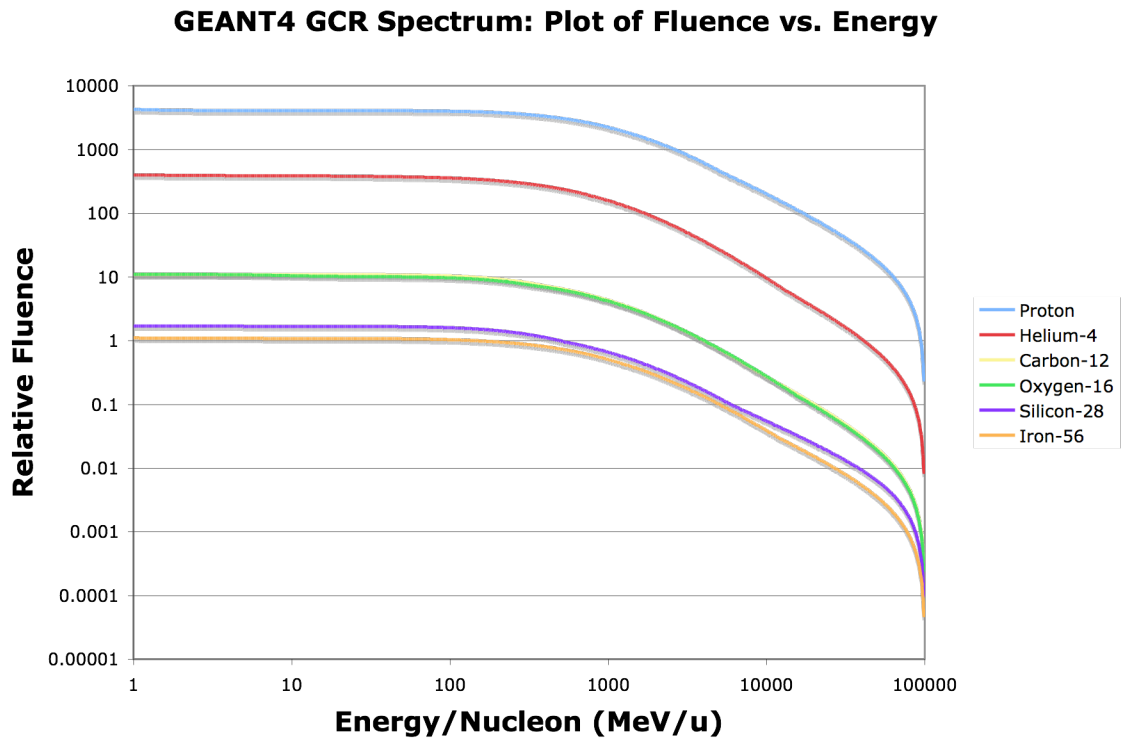

Figure 15. GEANT4's default GCR spectrum, which was used for the calculation in this paper.

By comparing this to HZETRN's GCR spectrum shown in figure 5, one can see that there is a very different shape to the curves. It should also be noted that this input spectrum is normalized in the code to the same number of GCR ions as were used in HZETRN, which is why the y-axis is labeled as a relative fluence. Unfortunately, there was not sufficient time to go back and change the GCR spectrum to HZETRN's spectrum and to use that to make a more direct comparison, and so the data determined with GEANT uses the spectrum shown in figure 15. The procedure described above along

with the GCR spectrum shown in figure 15 was used to make a GCR dose depth curve using GEANT, which is shown in figure 16.

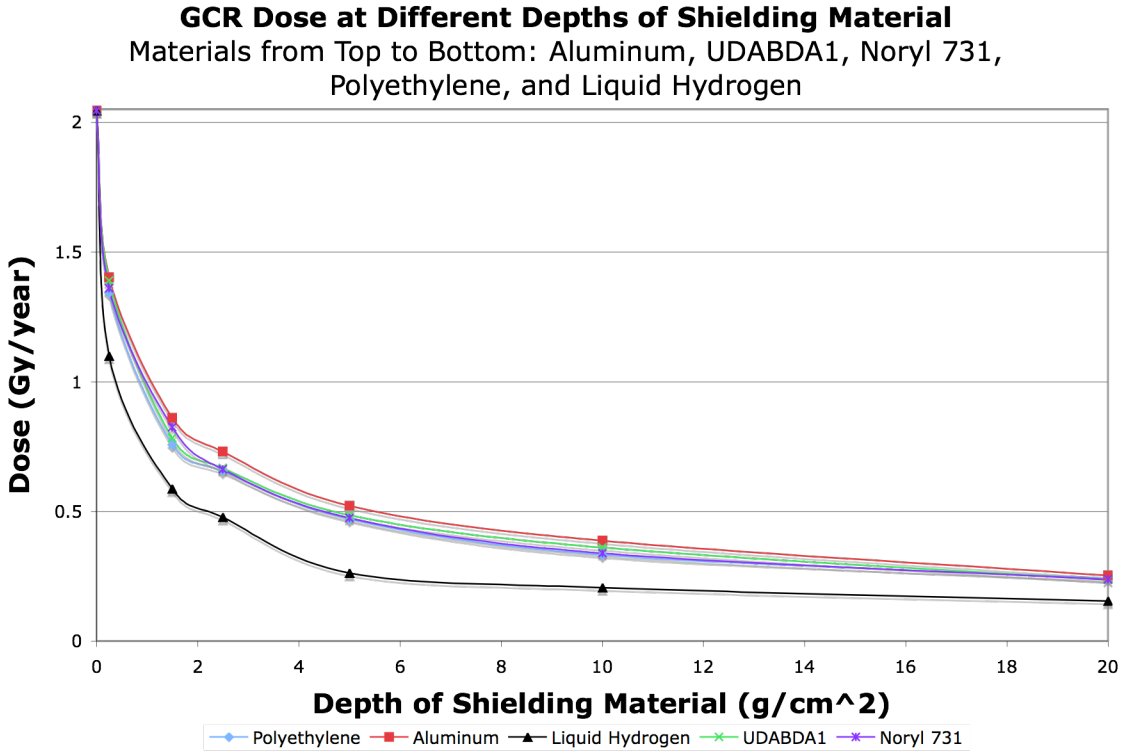

Figure 16. GEANT based GCR Dose Depth Curve for various Shielding Materials.

Figure 16 is slightly easier to see with the dose plotted on a logarithmic scale, as shown in figure 17.

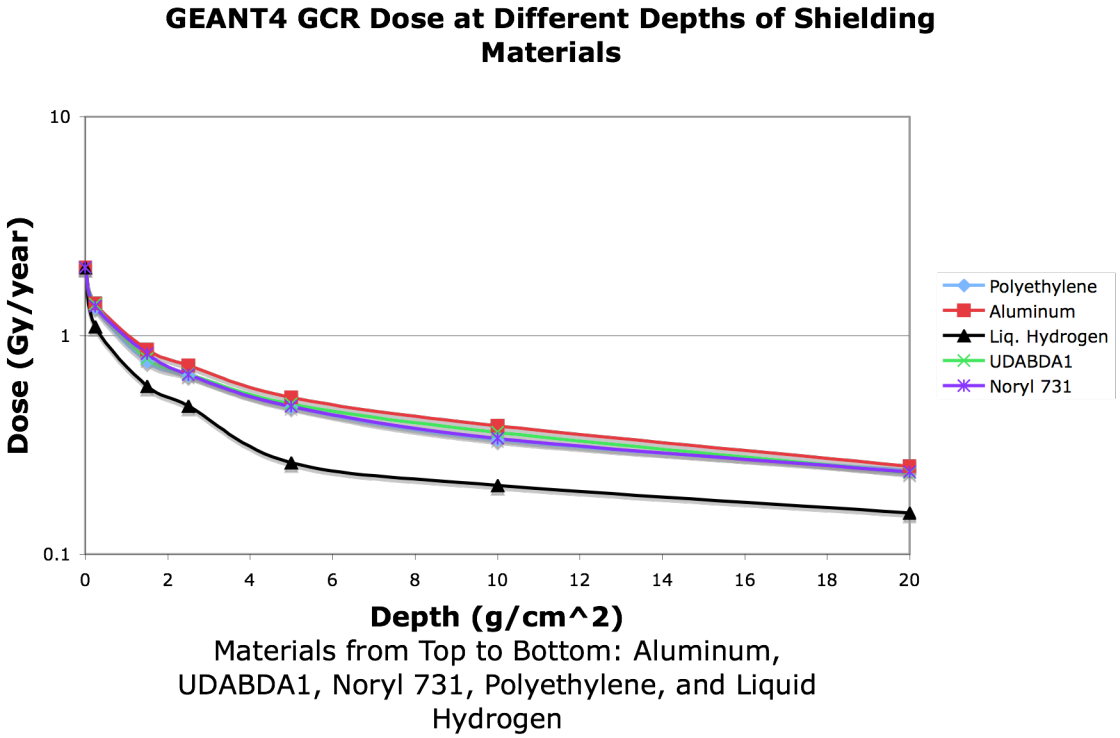

Figure 17. GEANT4 based GCR Dose Depth Curve on a log scale for various Shielding Materials.

This data replicates the same rank order of the shielding materials as HZETRN predicts it, which is good. However, the dose simply falls off far too quickly. It should not be falling off exponentially as shown, and this is a major problem, which could not be fixed. This is another possible future project. The fundamental physical processes handling fragmentation in GEANT will have to be changed to accurately model the physical interactions and produce reasonable results.

This major discrepancy between GEANT and HZETRN can be seen by looking at figure 18. Figure 18 shows a comparison between the predictions for Martian regolith by HZETRN and polyethylene by GEANT4. It is clear that the discrepancy is huge. While there was no available data for polyethylene or other materials simulated using GEANT4,

the results for Martian regolith should have the same shape of the curve as any other material. The only difference should be a vertical shift on the curve. There are two separate major problems with these results. First, the GCR dose with no shielding material is about a factor of ten too high. This is further evidence that 1 cm deep water is not correct. Reducing the thickness of water should decrease the GCR dose with no shielding material. The other major problem is that the shape of the curve is incorrect. As already explained, this is probably a problem with the modeling of fragmentation. There is clearly not enough fragmentation being produced in this GEANT4 code. This is another area for future work, which could also include tweaking the thickness of the water to obtain the correct dose with no shielding material. However, due to time constraints, this project was not able to complete that work. It is also not known how much of a problem the different input spectra are. The difference in input spectra may also partially account for the difference in results and may significantly narrow the gap between the results from GEANT and the results from HZETRN.

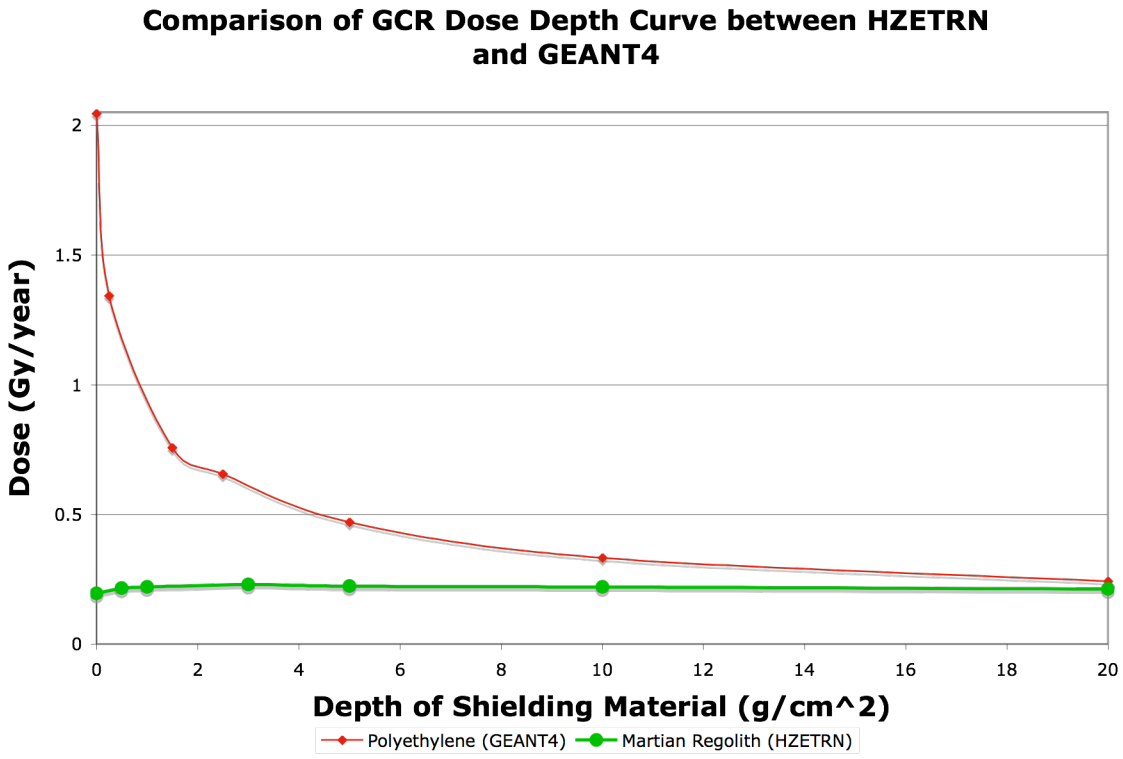

Figure 18. GCR Dose Depth Curve Comparison between GEANT4 and HZETRN.

Another possible future project could include extending this project's GEANT based code to include a means for calculating the dose equivalent as opposed to just dose. Furthermore, this code could be expanded to make comparisons against GRNTRN. It would be very interesting to see if GEANT could replicate the experimental results produced at Brookhaven. This would not be extremely difficult, since this code can already record the energy deposited in a user-specified material and can generate a beam of ions at constant energy. Therefore, one would only have to change the geometry to account for the different experimental setup.

Conclusions

This research has characterized some of the radiation shielding properties of certain polymers by using the NASA-Langley deterministic transport codes. It has been used to draw conclusions about which types of polymers may be particularly useful for shielding against radiation in space. Furthermore, this project has started work on a project to make comparisons between the NASA-Langley codes and GEANT4 with the hope that the NASA's results can be duplicated. This component of the project has not been completed but is still an ongoing project. However, there are some promising results that have been produced by GEANT4 modeling SPEs that suggest a high level of confidence in HZETRN. With any luck, that same level of confidence will emerge for the GCR spectrum as some of the remaining difficulties are solved.

Finally, there are still many unresolved technical problems associated with prolonged manned space flight beyond the van Allen belts. This research illustrates the difficulty in providing firm answers to many questions, because there are still so many unsolved questions. This project has also attempted to provide a few small answers to some of the outstanding questions so that future manned space flight will be less dangerous. However, as it should be clear, this project has attempted to answer a very limited number of these questions, showing the need for more future research on radiation shielding technologies.

References

1. Wilson, J.W., Miller, J., Konradi, A., and Cucinotta, F.A., Eds. "Executive Summary." Shielding Strategies for Human Space Exploration. NASA Conference Publication 3360. 1997. vii – x.

2. Wilson, J.W., Miller, J., Konradi, A., and Cucinotta, F.A., Eds. "Preliminary Considerations." Shielding Strategies for Human Space Exploration. NASA Conference Publication 3360. 1997. 3-15.

3. Wilson, J.W., Miller, J., Konradi, A., and Cucinotta, F.A., Eds. "Radiation Shielding Design Issues." Shielding Strategies for Human Space Exploration. NASA Conference Publication 3360. 1997. 111-149.

4. Fire Away, Sun and Stars! Shields to Protect Future Space Crews. National Aeronautics and Space Administration. 1/14/04. Accessed: 3/20/06. <http://www.nasa.gov/vision/space/travelinginspace/radiation_shielding.html>.

5. Radiation Shielding in Space. Health Physics Society. 10/7/05. Accessed: 3/20/06. <http://www.hps.org/publicinformation/ate/q4856.html>.

6. Segré, Emilio. "The Passage of Radiations Through Matter." Nuclei and Particles. New York: W. A. Benjamin, Inc., 1965. 17-77.

7. Personal Communication, Steve Blattnig, Ph.D., NASA-Langley Research Center.

8. Personal Communication, Steve Walker, Ph.D., NASA-Langley Research Center.

9. Introduction to GEANT4. GEANT4 Homepage. Accessed: 3/26/06. <http://geant4.web.cern.ch/geant4/G4UsersDocuments/Welcome/IntroductionToGeant4/html/introductionToGeant4.html#1>.

10. GEANT Physics Reference Manual- Decay. GEANT4 Homepage. Accessed 4/11/06. <http://geant4.web.cern.ch/geant4/G4UsersDocuments/UsersGuides/PhysicsReferenceManual/html/node12.html>.